PHOTOPRODUCTION OF NEUTRAL MESONS IN THE FIRST AND SECOND RESONANCE REGION*

B. KRUSCHE

II Physikalisches Institut, University of Giessen
D-35392 Giessen,Germany

(Received October 9, 1996)

The results from a series of experiments investigating π^0- and η-photoproduction are summarized. They were carried out with the TAPS detector at the Mainz MAMI accelerator. The p(γ,η)p reaction was used to study the excitation of the $S_{11}(1535)$ on the free nucleon. Quasifree η-photoproduction on deuterium was explored for a comparison of the p(γ,η)p and n(γ,η)n cross sections. These data together with an upper limit for the d(γ,η)d reaction allowed a determination of the electromagnetic helicity amplitudes of the $S_{11} \rightarrow N$ transition. Quasifree η-photoproduction on nuclei was used for a study of η nucleus final state interactions and the excitation of the $S_{11}(1535)$ resonance in the nuclear medium. Finally a comparison of free and quasifree π^0-production from the proton, the deuteron and from ^{12}C shows a strong suppression of the resonance structure for nuclear targets.

PACS numbers: 13.60. Le, 13.60. -r

1. Introduction

The basis for the description of electromagnetic and strong decays of <u>*free*</u> nucleon resonances in the quark model with chromodynamics was laid by the work of Koniuk and Isgur [1]. More recently, this program attracted again much interest because the new electron accelerators MAMI in Mainz, ELSA in Bonn and CEBAF in Newport News (USA), offer the opportunity for a new generation of very precise experiments. Therefore different groups (see *e.g.* [2–5]) revived and extended the quark model predictions of the baryon decay widths, preparing the ground for an extensive comparison to experiment.

In the case of <u>*bound*</u> nucleons even properties like mass and width are mostly unknown. Photoexcitation offers the advantage that due to the

---

* Presented at the "Meson 96" Workshop, Cracow, Poland, May 10–14, 1996.

small absorption probability of photons the complete volume of the atomic nucleus may contribute. This advantage may be partly lost due to final state interaction effects if exclusive reaction channels like meson production are used.

Photoproduction of η-mesons offers a very selective tool for the study of isospin $I = 1/2 N^{\star}$ resonances, because the $I = 3/2$ Δ-resonances cannot decay by emission of the isoscalar η-meson. All nucleon states in the second resonance region ($P_{11}(1440)$, $D_{13}(1520)$, and $S_{11}(1535)$) have branching ratios for the πN-channel on the order of 50 %. However, the $S_{11}(1535)$ has a very peculiar feature. The branching ratio for $S_{11}(1535) \rightarrow N\eta$ ($\approx$50%) is much larger than for any of the other resonances. The much weaker coupling of the neighboring P_{11} and D_{13} resonances can be explained by simple phase space arguments because they must decay to an $N\eta$ final state with relative orbital angular momentum $l = 1, 2$ which is strongly suppressed close to threshold. However, also the second S_{11} resonance at an excitation energy of 1655 MeV, has a branching ratio for η-decays only at the 1 % level or less. The quark models can explain this unusual pattern only by a strong mixing between the two resonances, however, even taking into account the mixing effects the widths are not well reproduced [1]. The situation was even more confusing for the electromagnetic transition amplitude $A_{1/2} = \langle S_{11} | j_{em} | N \rangle$ to the nucleon ground state. The quark models [1–4] and multipole analyses of pion photoproduction [6–9] agree that the electromagnetic excitation is dominated by an isovector transition. However, the absolute value of the amplitude predicted by the models is about twice as large as the result of the multipole analyses. A measurement of coherent η-photoproduction from deuterium found an unexpected large cross section [12] which requires a dominant isoscalar contribution to the transition amplitude. Consequently, the experimental results from pion and η-production are in contradiction and both do not agree with the quark model predictions. The detailed understanding of the elementary process of resonance excitation on the free nucleon is the basis for the investigation of resonance excitation in the nuclear medium. Recently, measurements of the total photoabsorption cross section [13, 14] showed a strong depletion of the resonance structure in the second resonance region. Total photoabsorption has the advantage, that no final state interaction effects are present. However, many different reaction channels (see figure 1) do contribute. In the region of interest a considerable fraction of the strength is due to the phase space opening of double pion production. It is therefore desirable to investigate the resonances in this region with exclusive experiments. The most selective reaction in this respect is photoproduction of η-mesons as a probe for the $S_{11}(1535)$ resonance.

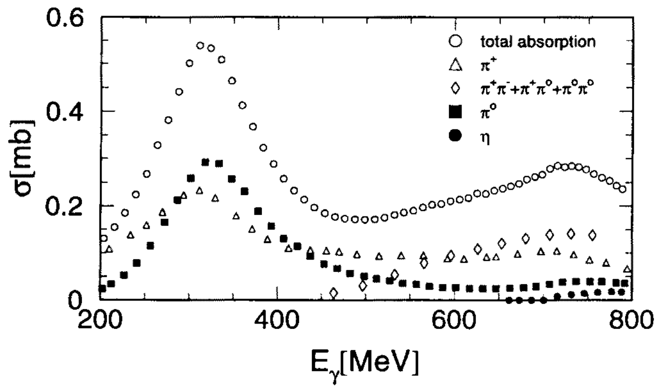

Fig. 1. Total cross section for photoabsorption on the proton and individual reaction channels of meson production. The data are from measurements at the MAMI accelerator with the DAPHNE detector (open symbols), and the TAPS detector (full symbols).

2. Experiments

An overview of the experimental program of TAPS in Mainz is given in [18]. Details of the experimental setup and the analysis procedures including time-of-flight-, pulse-shape-, invariant mass- and kinematical analyses exploring the kinematical overdetermination of the reactions can be found *e.g.* in Ref. [18, 31].

3. Results

The total cross section for the p(γ,η)p-reaction was determined from three independent reaction channels (see Fig. 2) namely the 2γ-decay of the η-meson and its $3\pi^0$-decay with 3 or 4 photons detected (see Refs [15, 16]) In this way, a very good control over systematical errors was achieved and as by-products precise values of the $\Gamma_{\eta\rightarrow 2\gamma}/\Gamma_{\eta\rightarrow 3\pi^0}$ branching ratio and the mass of the η-meson were obtained [16].

The average of the total cross section from all channels is compared to other data in figure 3. The old data base of the $p(\gamma,\eta)p$-reaction at energies below 900 MeV was measured with untagged Bremstrahlung experiments about 25 years ago. The result from a bubble chamber measurement [19] is shown in figure 3 as an example of this set of experiments. More recent results above 800 MeV were reported from Tokyo [10], but the experiment was restricted to η-emission angles in the range 80° - 115°. Also shown in figure 3 is the result of a measurement of η-electroproduction close to the photon point at the ELSA accelerator [22].

Simultaneously with the present work two new measurements of near threshold η-photoproduction have been published. Price *et al.* [20] measured the total cross section at energies below 720 MeV at the tagged photon beam of the ELSA accelerator. Their results are consistent with our measurement. Dytman *et al.* [21] measured total and differential cross sections using an untagged photon beam at the MIT-Bates linear accelerator. Their total cross section at the higher energy is in agreement with our results, but the two data sets disagree at the lower energy. Dytman *et al.* argue that the energy dependence of the cross section is inconsistent with the Breit–Wigner shape of a single s-wave resonance. However, this possibility is completely ruled out by our data, which as demonstrated in the figure, is in excellent agreement with the Breit–Wigner shape of an isolated resonance.

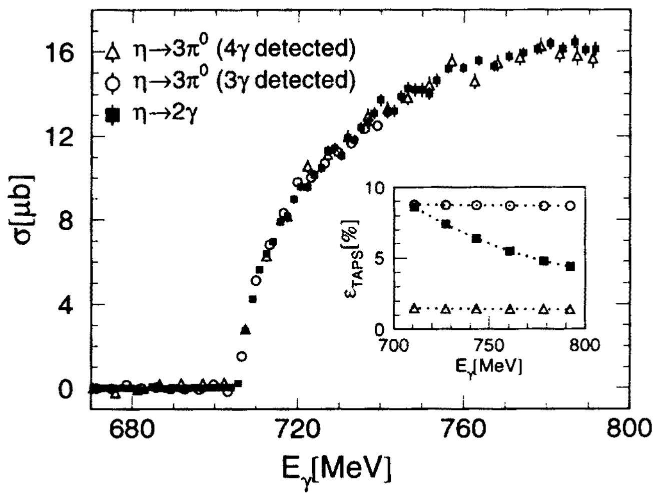

Fig. 2. Total cross section for the reaction $p(\gamma,\eta)p$. The data measured for the different decay channels of the η-meson are indicated. The insert shows the detection efficiency for these channels using the same symbols.

The combined analysis of the total cross section and the angular distributions which are rather flat and the comparison to the results from various model calculations gave the following results [15, 18]:

- The total cross section below 800 MeV is completely dominated by the $S_{11}(1535)$-resonance. The contribution of other resonances, nucleon Born terms and vector meson exchange is vanishingly small. In the

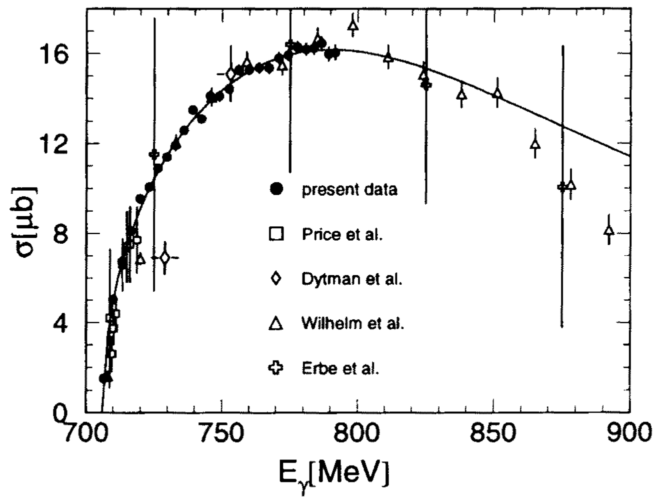

Fig. 3. Comparison of the total cross section for the reaction $p(\gamma,\eta)p$ [15] to the data from Erbe *et al.* [19], Price *et al.* [20], Dytman *et al.* [21] and Wilhelm *et al.* [22]. The solid line shows a Breit–Wigner fit to the present data.

models not all non-S_{11} contribution are negligible, however those which are not negligible cancel each other.

- A small contribution of the $D_{13}(1540)$-resonance could be identified in the angular distributions via an interference with the leading S_{11}-term.
- Comparison to model predictions shows a preference for a pseudoscalar coupling with a small coupling constant ($g_\eta^2/4\pi \approx 0.5$) at the ηNN vertex in the nucleon Born terms.

The total cross section was fitted with a Breit–Wigner curve using

$$\frac{k^\star}{q_\eta^\star}\sigma(W) = \frac{AW_R^2\Gamma_R^2}{(W_R^2 - W^2)^2 + W_R^2\Gamma(W)^2}\,, \tag{1}$$

where $W = \sqrt{s}$ is the total cm energy, W_R and Γ_R are the resonance position and width, respectively, and the energy dependent width

$$\Gamma(W) = \Gamma_R\left(b_\eta\frac{q_\eta^\star}{q_{\eta R}^\star} + b_\pi\frac{q_\pi^\star}{q_{\pi R}^\star} + b_{\pi\pi}\right) \tag{2}$$

is needed because the resonance is located very close to the η-production threshold. This width is parametrized in terms of the η and π cm momenta

$q_\eta^\star$, $q_\pi^\star$, the respective momenta at resonance, and the S_{11} decay branching ratios b_η, b_π, and $b_{\pi\pi}$. The branching ratios are not well known (b_η=0.3 - 0.55, b_π=0.35 - 0.55, $b_{\pi\pi} \leq 0.1$ [27]). We have therefore performed three different fits, spanning the parameter range. In the absence of significant contributions from other multipoles, the E_{o+}-amplitude is related to the total cross section via:

$$|E_{o+}(W)| = \left(\frac{1}{4\pi}\frac{k^\star}{q_\eta^\star}\sigma(W)\right)^{1/2} \tag{3}$$

and the electromagnetic helicity coupling $A_{1/2}$ follows from [15]:

$$A_{1/2} = \left(\frac{W_R}{2m_p}\right)^{1/2}\left(\frac{\Gamma_R}{b_\eta}\right)^{1/2}\sigma(W_R)^{1/2}. \tag{4}$$

The helicity coupling depends on the poorly known hadronic widths of the η-meson and therefore it was suggested in [11] to use instead the 'electrostrong' coupling ξ defined by

$$\xi = \left(\frac{k^\star}{q_\eta^\star}\right)^{1/2}\left(\frac{m_p}{W_R}\right)^{1/2}\left(\frac{b_\eta}{\Gamma_R}\right)^{1/2} A_{1/2} = \sqrt{2\pi}|E_{o+}(W_R)| \tag{5}$$

for a comparison to model predictions. The results obtained from the Breit–Wigner fits are summarized in Table I.

TABLE I

S_{11} parameters from Breit-Wigner fits (Fit 1: b_η=0.55, b_π=0.35, Fit 2: b_η=0.45, b_π=0.45, Fit 3: b_η=0.35, b_π=0.55).

		Fit 1	Fit 2	Fit 3	PDG
W_R	[MeV]	1549±8	1544±8	1539±8	1520-1555
Γ_R	[MeV]	202±35	203±35	208±35	100-250
$\|E_{o+}^p(E_{\text{thr}})\|$	$[10^{-3}/m_{\pi^+}]$	16.14	16.08	16.05	
$\Re(E_{o+}^p(E_{\text{thr}}))$	$[10^{-3}/m_{\pi^+}]$	13.4	12.0	10.3	
$\Im(E_{o+}^p(E_{\text{thr}}))$	$[10^{-3}/m_{\pi^+}]$	9.0	10.7	12.3	
$\|E_{o+}^p(W_R)\|$	$[10^{-3}/m_{\pi^+}]$	12.03	12.34	12.66	
$A_{1/2}^p$	$[10^{-3}GeV^{-1/2}]$	112±3	124±3	142±4	68±10
ξ^p	$[10^{-4}MeV^{-1}]$	2.16±0.06	2.22±0.06	2.27±0.06	

A study of the isospin structure of the S_{11}-resonance requires a measurement of η-photoproduction from a neutron target. The only possibility for such an experiment is quasifree photoproduction from light nuclei, in particular from the deuteron. The measured total cross section for quasifree η-production is shown in figure 4. It is compared to the free proton data in order to extract the neutron cross section. The present data were modelled using the Breit–Wigner fit of the proton cross section which was then folded with the nucleon Fermi motion by a Monte Carlo calculation [17, 18]. Best agreement was obtained for a constant ratio of the neutron and proton cross section of $\sigma_n/\sigma_p = 2/3$, which reproduced not only the measured total cross section on the deuteron but also angular and momentum distributions [18]. The largest systematic uncertainty arises from the assumptions made in the participant - spectator approximation and this is expected to contribute at the 10 % level. An analysis of the data in the framework of a coupled channel model by Sauermann *et al.* [24], which is also shown in figure 4, gave the same result.

From the ratio of neutron and proton cross section we may derive the E_{o^+}-amplitude at resonance for the neutron via:

$$|E^n_{o^+}(W_R)| = \sqrt{\sigma_n/\sigma_p}|E^p_{o^+}(W_R)|\,. \tag{6}$$

Using the values from Table I we obtain:

$$|E^n_{o^+}(W_R)| = (10.0 \pm 0.6)10^{-3}/m_{\pi^+} \tag{7}$$

in which a 10 % error for the extraction of σ_n/σ_p is included.

The ratio of the isovector and isoscalar parts is obtained from:

$$\left(\frac{E^{IV}_{o^+}}{E^{\mathrm{IS}}_{o^+}}\right)^{\pm 1} = \left[\frac{1+\sqrt{\sigma_n/\sigma_p}}{1-\sqrt{\sigma_n/\sigma_p}}\right] = (10 \pm 2.5)\,, \tag{8}$$

where the exponent depends on the relative sign of $E^p_{o^+}(W_R)$ and $E^n_{o^+}(W_R)$. The data supports the finding that either the isoscalar or the isovector part of the S_{11}-excitation is small. Which component is the dominating one is decided by coherent η-production on the deuteron.

In the present experiment the separation of quasifree and coherent photoproduction was achieved by means of missing energy or missing momentum analyses. In the case of coherent η-production from the deuteron an upper limit of the cross section of (1 ± 10)nb/sr at an average photon energy of 685 MeV and for a cm angle of $\Theta_\eta = 90°$ was deduced [17, 18], which is considerably smaller than the value reported earlier by Anderson *et al.* [12] ((37 ± 5)nb/sr). This small cross section rules out a dominant

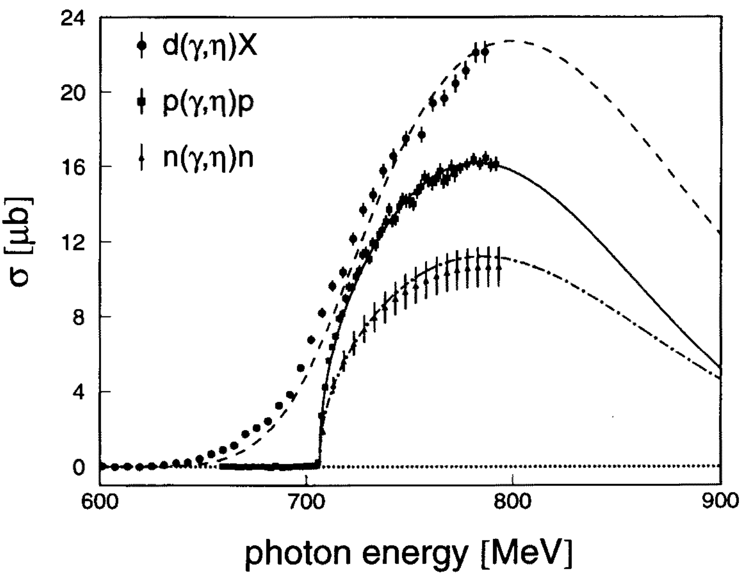

Fig. 4. Total cross sections of the $p(\gamma,\eta)p$-, $d(\gamma,\eta)np$- and $n(\gamma,\eta)n$-reactions. The values for the $n(\gamma,\eta)n$-reaction are the measured proton cross section scaled by a factor of 0.66. The coupled channel calculations of Sauermann *et al.* [24] are represented by the dashed, solid and dash-dotted lines.

isoscalar excitation of the S_{11}-resonance and thus implies a positive relative sign between the helicity amplitudes from the proton and the neutron.

The final results for the helicity amplitudes are summarized in Table II.

TABLE II

Electromagnetic and 'electrostrong' coupling constants of the $S_{11}(1535)$ resonance from different analyses of the present data compared to other experimental results and quark model predictions. The values for $A_{1/2}$ are in units of $[10^{-3}\text{GeV}^{-1/2}]$, the values for ξ in units of $[10^{-4}\text{MeV}^{-1}]$.

Ref.	Meth.*)	$A^p_{1/2}$	$A^n_{1/2}$	$A^n_{1/2}/A^p_{1/2}$	ξ^p	ξ^n
tw†	A	125±25	−100±30	−0.81±0.05	2.22±0.15	−1.80±0.15
[23]	A	98	−82	−0.84±0.15	2.20±0.15	−1.86±0.20
[24]	A	102	−82	−0.80	2.24	−1.79
[25]	A	111			2.20	
[26]	A	107				
[10]	B	133^{+55}_{-39}				
[28]	B			±1.0		
[12]	B			+1.0		
[6]	C	63±13	−51±21	−0.8		
[7]	C	80±7	−75±18	−0.9		
[8]	C	65±16	−98±26	−1.5		
[9]	C	61±3	−46±5	−0.75		
[29]	D	156	−108	−0.7		
[6]	D	166	−116	−0.7		
[1]	D	147	−119	−0.8		
[2]	D	163	−106	−0.65		
[4]	D	54	−57	−1.06		
[30]	D	127	−103	−0.8		

*) A: η-photoproduction (present data), B: η-photoproduction (other experiments) C: pion photoproduction, D: predictions from quark models
† tw: this work

The values obtained from the present data by different analyses are compared to other η-photoproduction experiments, to the results from multipole analyses of pion photoproduction, and to quark model predictions. The following remarks can be made to Table II:

- All analyses of the present data produce very similar values for the 'electrostrong' coupling ξ reflecting its independence of the hadronic widths and the strong dominance of the $S_{11}(1535)$ resonance.
- The different absolute values of the helicity couplings from the analyses of the present data are due to the used hadronic widths of the S_{11}-resonance.
- The absolute value and the sign of the ratio of the helicity couplings is in good agreement with pion multipole analyses and quark model predictions.
- The absolute values of the helicity couplings from η-photoproduction are significantly larger than the results from pion photoproduction. The S_{11}-resonance contributes only very weakly to pion photoproduction, so that the extraction of the coupling requires a complicated multipole analysis. There is already some indication that the discrepancy is due to problems of the extraction of the couplings from the pion data. The more elaborate coupled channel analysis of elastic pion scattering, pion induced η-production, and π-, η-photoproduction by Sauermann *et al.* finds a consistent description of all processes with a coupling of $A^p_{1/2}$=102×10^{-3}GeV$^{-1/2}$.

The results for the total cross section of η-photoproduction from nuclei are summarized in figure 5 and compared to the cross section on the proton and the deuteron. The figure shows that the probability of observing an η-meson per nucleon is largely reduced for the nuclear targets not only with respect to the proton but also with respect to the deuteron. The decrease of the cross section for the heavier nuclei points to final state interaction effects, in particular reabsorption of the η-mesons. The cross section should scale like the mass number if the mean free path for η-mesons in nuclear matter is large compared to the nuclear radii.

If, on the other hand, the mean free path is small compared to the nuclear radii we expect that the cross section scales like the nuclear surface, *i.e.* like $A^{2/3}$. We have fitted the A-dependence of the cross section for the nuclear targets with an ansatz:

$$\sigma(A, E_\gamma) \propto A^{\alpha(E_\gamma)}\,. \tag{9}$$

The data and the fits are shown in figure 6. The measured cross sections are in quite good agreement with an A^α-scaling law and the fitted exponents are close to 2/3 without any significant energy dependence. The data have been analysed [31] in the framwork of the Glauber approximation which gave an absorption cross section of

$$\sigma^{\text{abs}}_{\eta N} = (30 \pm 2.5 \pm 6.0)\text{mb} \tag{10}$$

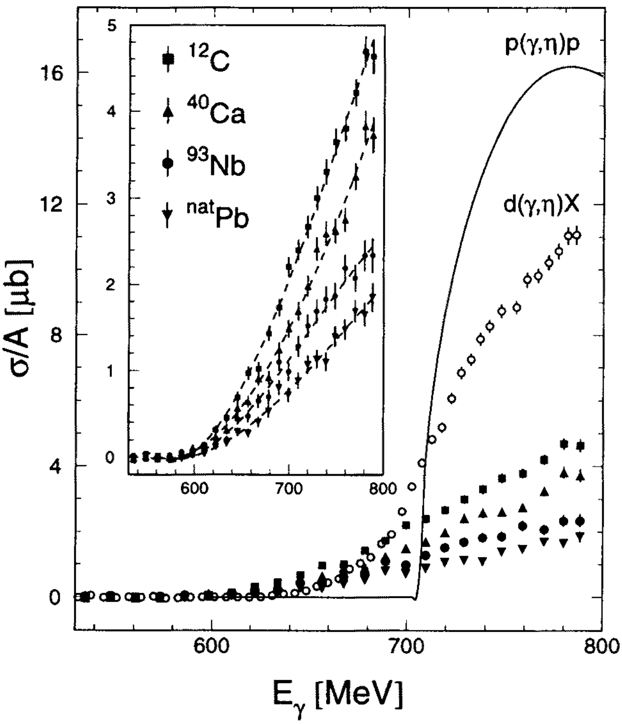

Fig. 5. Total cross section scaled by the mass number of the nuclei as function of incident photon energy. The Breit-Wigner fit for the proton data is shown for comparison. The insert shows the nuclear data on an enlarged scale. The dashed lines in the insert should only help to guide the eye [31].

corresponding to a mean free path of η-mesons in nuclear matter of:

$$\lambda_\eta = (2.0 \pm 0.2 \pm 0.4)\,\text{fm}\,. \tag{11}$$

Consequently, η-mesons have only a small chance to escape from the interior of the nucleus but will mainly be emitted from the surface region. A comparison to the predictions from a BUU-model calculation [33] showed that the most probable production region of observed η-mesons is centered around half the mean nuclear density. The data were compared to the predictions from various models [33–35] which reproduced them quite well taking into account effects of Fermi smearing, Pauli blocking and final state interaction effects. No significant medium modifications of the resonance and in particular no unexplained depletion of its strength in nuclear matter were observed [31, 32, 18]. However, one must keep in mind that due to the final state interaction nuclear matter was tested at $\approx 1/2\ \rho_o$ which corre-

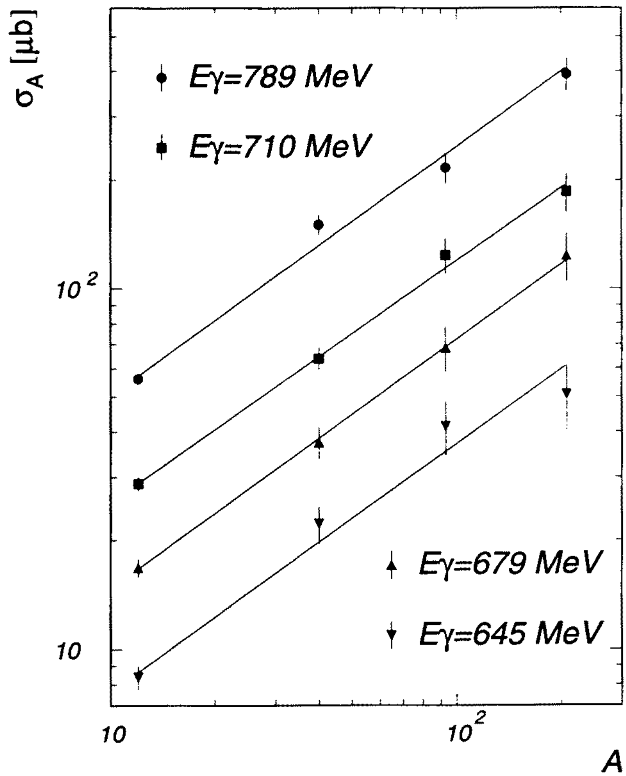

Fig. 6. Total cross sections for η-production from nuclei as function of the mass number for different incident photon energies. The data have been fitted by an A^{α}-ansatz (solid lines) [31].

sponds to the most probable production region of observed η-mesons. On the other hand the strong depletion of the cross section in the D_{13}-region is observed by total photoabsorption already for nuclei as light as beryllium, lithium and carbon where the probed average density is also low. The damping of the cross section in the D_{13}-region is practically independent from the mass number which argues against a strong density dependence. Consequently, we can conclude that at least the $S_{11}(1535)$ resonance is not strongly affected by the overall damping of the cross section observed in the photoabsorption experiments.

The situation is less clear for the $D_{13}(1520)$ resonance which is observed in pion photoproduction. The comparison of the data from the deuteron and from carbon (see figure 7) indeed shows a strong reduction of the cross section in the D_{13}-region which might be more in line with the results from the photoabsorption experiments. However, a quantitative analysis of this effect again requires the comparison to models which account for the trivial effects of Fermi smearing and final state interactions. Such calculations in the framework of the BUU model are under way.

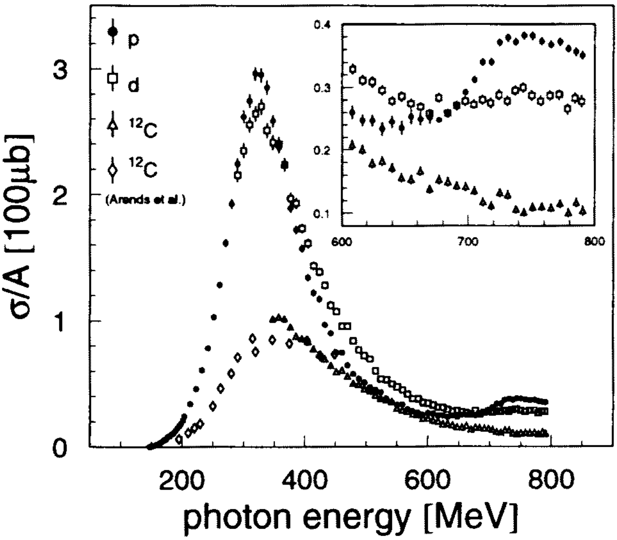

Fig. 7. Total cross section for quasifree π^o-photoproduction from the proton, deuteron and from ^{12}C scaled by the mass number versus incident photon energy. The low energy data for pion production from carbon is taken from [36]. The insert shows the second resonance region on an enlarged scale.

REFERENCES

[1] R. Koniuk, N. Isgur, *Phys. Rev.* **D21**, 1868 (1980).
[2] F.E. Close, Z. Li, *Phys. Rev.* **D42**, 2194 (1990).
[3] Z. Li, F.E. Close, *Phys. Rev.* **D42**, 2207 (1990).
[4] M. Warns, W. Pfeil, H. Rollnik, *Phys. Rev.* **D42**, 2215 (1990).
[5] S. Capstick, W. Roberts, *Phys. Rev.* **D49**, 4570 (1994).
[6] W.J. Metcalf, R.L. Walker, *Nucl. Phys.* **B76**, 253 (1974).
[7] I. Arai, H. Fujii, *Nucl. Phys.* **B194**, 251 (1982).
[8] R.L. Crawford, W.T. Morton, *Nucl. Phys.* **B211**, 1 (1983).
[9] R.A. Arndt *et al.*, *Phys. Rev.* **C42**, 1853 (1990); Z. Li *et al.*, *Phys. Rev.* **C47**, 2759 (1993).
[10] S. Homma *et al.*, *J. Phys. Soc. Jpn.* **53**, 828 (1988).
[11] M. Benmerrouche *et al.*, *Phys. Rev.* **D51**, 3237 (1995).

[12] R.L. Anderson, R. Prepost, *Phys. Rev. Lett.* **23**, 46 (1969).

[13] Th. Frommhold *et al.*, *Phys. Lett.* **B295**, 28 (1992).

[14] N. Bianchi *et al.*, *Phys. Lett.* **B299**, 219 (1993).

[15] B. Krusche *et al.*, *Phys. Rev. Lett.* **74**, 3736 (1995); B. Krusche *et al. Phys. Rev. Lett.* **75**, 3023 (1995).

[16] B. Krusche *et al.*, *Z. Phys.* **A351**, 237 (1995).

[17] B. Krusche *et al.*, *Phys. Lett.* **B358**, 40 (1995).

[18] B. Krusche, Habiltationsschrift, University of Giessen, (1995), (unpublished).

[19] R. Erbe *et al.*, (ABBHHM collaboration) *Phys. Rev.* **175**, 1669 (1968).

[20] J.W. Price *et al.*, *Phys. Rev.* **C51**, R2283 (1995).

[21] S.A. Dytman *et al.*, *Phys. Rev.* **C51**, 2710 (1995).

[22] M. Wilhelm, PhD thesis, University of Bonn (1993) (unpublished).

[23] N.C. Mukhopadhyay *et al.*, *Phys. Rev. Lett* **75**, 3022 (1995); N.C. Mukhopadhyay *et al.*, *Phys. Lett.* **B364**, 1 (1995).

[24] Ch. Sauermann *et al.*, *Phys. Lett.* **B341**, 261 (1995). Ch. Sauermann *et al.*, Proc. of the VI Int. Symp. on Meson-Nucleon Physics and the Structure of the Nucleon, Blaubeuren, Germany, July 1995, and priv. com.

[25] Z. Li, *Phys. Rev.* **D** accepted.

[26] G. Knöchlein *et al.*, *Z. Phys.* **A352**, 327 (1995).

[27] L. Montanet *et al.*, *Phys. Rev.* **D50**, (1994). *Review of particle properties* !?!!?

[28] C.Bacci *et al.*, *Phys. Lett.* **B28**, 687 (1969).

[29] R.P. Feynman *et al.*, *Phys. Rev.* **D3**, 2706 (1971).

[30] R. Bijker *et al.*, *Ann. Phys.* **236**, 69 (1994).

[31] M.E. Röbig-Landau, PhD thesis, University of Giessen, (1995) (unpublished).

[32] M. Röbig-Landau *et al.*, *Phys. Lett.* **B358**, 40 (1996).

[33] A. Hombach *et al.*, *Z. Phys.* **A352**, 223 (1995) and private communication.

[34] R.C. Carrasco, *Phys. Rev.* **C48**, 2333 (1993).

[35] L. Tiator *et al.*, Proceedings of the XV European Conf. on Few Body Problems in Physics, June 5–9 1995, Peniscola, Spain (suppl. to Few Body Systems).

[36] J. Arends *et al.*, *Z. Phys.* **A 311**, 367 (1983).